



ELSEVIER

Signal Processing 38 (1994) 57–77

**SIGNAL
PROCESSING**

Morphological systems: Slope transforms and max–min difference and differential equations[†]

Petros Maragos*

School of Electrical and Computer Engineering, Georgia Institute of Technology, Atlanta, GA 30332-0250, USA

Received 21 September 1993; revised 10 December 1993

Abstract

Linear time-invariant systems are well understood in the time domain either as convolutions with their impulse response or by describing their dynamics via linear differential equations. Their analysis in the frequency domain using their exponential eigenfunctions and related frequency response is also greatly facilitated via Fourier transforms. Attempting to extend such ideas to nonlinear systems, we present in this paper a theory for a broad class of nonlinear systems and a collection of related analytic tools, which parallel the functionality of and have many conceptual similarities with ideas and tools used in linear systems. These nonlinear systems are time-invariant dilations or erosions, in continuous and discrete time, and obey a supremum- or infimum-of-sums superposition. In the time domain, their equivalence with morphological dilation or erosion by their impulse response is established, and their causality and stability are examined. A class of nonlinear difference and differential equations based on max–min operations is also introduced to describe their dynamics. After finding that the affine signals $\alpha t + b$ are eigenfunctions of morphological systems, their slope response is introduced as a function of the slope α , and related slope transforms for arbitrary signals are developed. These ideas provide a transform (slope) domain for morphological systems, where dilation and erosion in time corresponds to addition of slope transforms. Recursive morphological systems, described by max–min difference equations, are also investigated and shown to be equivalent to dilation or erosion by infinite-support structuring elements. Their analysis is significantly aided by using slope transforms. These recursive morphological systems are applied to the design of ideal-cutoff slope-selective filters which are useful for signal envelope estimation.

Zusammenfassung

Lineare zeitinvariante Systeme werden im Zeitbereich gut verstanden entweder als Faltungen mit deren Impulsantwort oder indem ihre Dynamik mit linearen Differentialgleichungen beschrieben wird. Ihre Analyse im Frequenzbereich durch die Verwendung ihrer exponentiellen Eigenfunktionen und der verwandten Frequenzantwort wird auch durch die Fouriertransformation sehr vereinfacht. Mit dem Ziel solche Ideen auch auf nichtlineare Systeme auszuweiten, präsentieren wir in diesem Artikel eine Theorie für eine umfangreiche Klasse von nichtlinearen Systemen und eine Sammlung von verwandten analytischen Werkzeugen, die die gleiche Funktionalität und viele konzeptuelle Ähnlichkeiten mit Ideen und Werkzeugen haben, die in linearen Systemen benutzt werden. Diese nichtlinearen Systeme sind zeitinvariante Dilatationen und Erosionen, zeitkontinuierlich oder zeitdiskret, und folgen einer Superposition von

[†]Early parts of this research work were partially supported by the US National Science Foundation under Grant MIP-86-58150. This paper was written while the author was supported by National Science Foundation under Grant MIP-91-20624.

* Tel: 404-894-3930. Fax: 404-894-8363. E-mail: maragos@ee.gatech.edu.

Supremum- oder Infimum der Summen. Im Zeitbereich wird ihre Gleichwertigkeit mit morphologischer Dilatation und Erosion durch ihre Impulsantworten hergestellt und deren Kausalität und Stabilität untersucht. Eine Klasse von nichtlinearen Differenzen- und Differentialgleichungen, die auf Max–Min-Operationen basieren, wird ebenfalls eingeführt, um ihre Dynamik zu beschreiben. Nachdem herausgefunden wurde, daß die affinen Signale $at + b$ Eigenfunktionen von morphologischen Systemen sind, wird ihre Steigung als Funktion der Steigung α eingeführt und verwandte Steigungstransformationen für beliebige Signale entwickelt. Diese Ideen liefern einen Transformationsraum (Steigung) für morphologische Systeme, wobei Dilatation und Erosion im Zeitbereich mit der Addition der Steigungstransformierten korrespondieren. Rekursive morphologische Systeme, beschrieben durch Max–Min Differenzgleichungen, werden ebenfalls untersucht und es wird gezeigt, daß sie gleichwertig mit Dilatation und Erosion durch endliche Strukturelemente sind. Ihre Analyse wird entscheidend durch Steigungstransformationen unterstützt. Diese rekursiven morphologischen Systeme werden für den Entwurf von steigungsselektiven Filtern mit einem idealen Cutoff angewendet, was für die Schätzung der Einhüllenden von Signalen nützlich ist.

Résumé

Les systèmes linéaires et invariants dans le temps sont bien compris dans le domaine temporel soit à l'aide de convolution soit en décrivant leur dynamique à l'aide d'équations différentielles. Leur analyse dans le domaine fréquentiel reposant sur les exponentielles complexes et la réponse fréquentielle est facilitée par l'existence de la transformation de Fourier. Dans le but d'étendre ces idées aux systèmes nonlinéaires, cet article présente une théorie pour une large classe de systèmes nonlinéaires ainsi qu'une série d'outils qui possèdent la même fonctionnalité et une grande similitude avec les outils utilisés pour les systèmes linéaires. Ces systèmes nonlinéaires sont des érosions et des dilatations invariantes dans le temps et obéissent à une loi de superpositions de supremum (ou infimum) de sommes. Dans le domaine temporel, leur équivalence avec les érosions et dilatations morphologiques est établie à l'aide de leur réponse impulsionnelle, de plus leur stabilité et causalité est examinée. Une classe d'équations différentielles et aux différences basées sur des opérations min–max est introduites pour décrire leur dynamique. Après avoir montré que les signaux affines $at + b$ sont des fonctions propres des systèmes morphologiques, leur réponse en 'pente' est introduite comme une fonction de la pente a et la transformation de pente pour des signaux arbitraires est développée. Ces idées débouchent sur un domaine transformé pour les systèmes morphologiques où les dilatations et les érosions correspondent à des additions des transformées en pente. Les systèmes morphologiques récursifs, définis par des équations différences min–max, sont également étudiés. On montre qu'il sont équivalents à des dilatations et des érosions avec des éléments structurants de taille infinie. Leur analyse est facilitée par l'utilisation de la transformée en pente. Ces systèmes morphologiques récursifs sont appliqués à la conception de filtres idéaux sélectif en pente qui sont utiles pour l'estimation d'enveloppe.

Key words: Morphological systems; Slope transforms; Max–min difference equations

1. Introduction

Morphological systems is a broad class of nonlinear signal operators that have found many applications in image analysis and nonlinear filtering. All morphological systems are based on parallel or serial interconnections of morphological dilations \oplus or morphological erosions \ominus [16, 18, 10],

$$x(t) \oplus g(t) = \bigvee_{\tau} x(\tau) + g(t - \tau), \quad (1)$$

$$x(t) \ominus g(t) = \bigwedge_{\tau} x(\tau) - g(\tau - t), \quad (2)$$

where \bigvee denotes supremum and \bigwedge denotes infimum. So far their analysis has been done only in

the time domain by using their algebraic properties and lacked a transform domain. Thus it lacked tools whose functionality would be similar to that of the tools available for linear time-invariant (LTI) systems. By contrast, LTI systems can be analyzed in the time domain either via linear differential equations or as convolutions via their impulse response, a signal that can also determine their causality and stability. Thanks to Fourier transforms which map signal convolution to transform multiplication, LTI systems can also be analyzed in a transform domain using their exponential eigenfunctions and related frequency response.

A major question/problem then arises: Can we endow morphological systems with similar analytic

tools that have found so much use in linear systems? The answer is *yes*: in this paper we introduce various concepts and analytic methods that enable us to uniquely determine the output and properties of these nonlinear systems in the time domain based solely on their *impulse response*. In addition, we develop nonlinear difference and differential equations that describe the time dynamics of these systems. Further, after finding that the line signals $at + b$ are *eigenfunctions* of morphological systems, we introduce a *slope response*, a function of the slope variable α , which enables us to understand the systems behavior in a transform domain – the slope domain. This nonlinear analysis leads to developing signal transforms called *slope transforms* whose properties and application to morphological systems have some striking conceptual similarities with Fourier transforms and their application to LTI systems. We study three types of slope transforms and their interrelationships: (i) a single-valued transform for signals processed by dilation systems and (ii) a dual transform for signals processed by erosion systems, both introduced by Maragos [8] to aid the analysis of morphological systems; (iii) a multivalued transform that results by replacing the suprema and infima of signals with values at stationary points, introduced by Dorst and Van den Boomgaard [4]. For continuous-time signals that are convex or concave and have an invertible derivative all three transforms coincide and become identical to the Legendre transform, which has found applications in various methods of mathematical physics [2, 3]. For discrete-time signals only transforms (i) and (ii) can be used, whereas the Legendre transform and its generalization (iii) cannot directly apply.

The applications of LTI systems include cases where their impulse response has support of either infinite or finite length. However, the vast majority of theory and applications of morphological signal processing assumes that the impulse response (e.g., the structuring element) involved has compact support. In discrete time, this implies that the moving max/min of additions takes place only over a finite window of input samples. There is, however, an important application that requires max/min operations by recursing on output samples. This occurs during the computation of the distance

transform of digital binary images [15, 1]; e.g., passing in forward time a discrete binary signal $x[n] \in \{0, \infty\}$ as input to the recursive equation

$$y[n] = \min(y[n-1] + 1, x[n]) \quad (3)$$

and then running the result through the same equation but backward in time creates as final output the distance transform of x , which is useful for image skeletonization, multiscale analysis, and segmentation [15, 16, 7]. In addition, recursive rank-order filters [12] of the type

$$y[n] = r^{\text{th}} \text{rank} \{y[n-N], \dots, y[n-1], x[n], x[n+1], \dots, x[n+N]\}, \quad 1 \leq r \leq 2N+1 \quad (4)$$

include recursive max and min operations as special cases. However, the max–min cases are the most important since any rank-order operation is a minimum of maxima or maximum of minima [10]. In this paper we introduce a theory for recursive dilations and erosions by modeling them via nonlinear difference equations of the max–min type. Whenever such an equation has a recursive part, we show that this corresponds to dilating the input signal with an infinite-support structuring function. Further, we derive many interesting results concerning the impulse response, causality, stability, and eigenfunctions of such systems by drawing analogies with similar properties of linear systems described by linear difference equations [14, 13]. Slope transforms are used to aid the analysis of recursive morphological systems and to design slope-selective filters that are useful for signal envelope estimation. Finally, we present a nonlinear differential equation which is the continuous-time version of the max difference equation and corresponds to a realizable ideal-cutoff slope filter.

2. Dilation translation-invariant (DTI) systems

A signal operator $\mathcal{D}: x \mapsto y = \mathcal{D}(x)$ is called a *dilation translation-invariant (DTI)* system if it distributes over the supremum of any collection $\{x_i\}$ of input signals, i.e., $\mathcal{D}(\bigvee_i x_i) = \bigvee_i \mathcal{D}(x_i)$ (i.e., if it is a ‘dilation’ in the lattice-based theory of mathematical morphology [17, 5]), and if it is translation-invariant, i.e., $\mathcal{D}[x(t-t_0) + c] =$

$c + [\mathcal{D}(x)](t - t_0)$ for any time shift t_0 and any real constant c . These two conditions together are equivalent to saying that a system is DTI if it is time-invariant and obeys the morphological *supremum superposition* principle

$$\mathcal{D}\left[\bigvee_i c_i + x_i(t)\right] = \bigvee_i c_i + \mathcal{D}[x_i(t)], \quad (5)$$

where $c_i \in \mathbb{R}$.

For (one-dimensional) DTI systems we assume input and output signals $x: E \rightarrow \bar{\mathbb{R}}$ whose domain E is equal to \mathbb{R} for continuous-time signals or to \mathbb{Z} for discrete-time signals, and whose range is any subset of $\bar{\mathbb{R}} = \mathbb{R} \cup \{-\infty, \infty\}$. The useful information in a signal x analyzed by a DTI system exists only at times t where $x(t) > -\infty$. Thus its *support* (or effective domain) is defined by $\text{Spt}(x) \triangleq \{t: x(t) > -\infty\}$.

Two important aspects of a DTI system are its causality and stability. A system is *causal* (respectively *anti-causal*) if its output value at each time instant depends only on present and/or past (respectively future) input values. A system is *stable* if an absolutely bounded (within its support) input signal x yields a bounded (within its support) output signal y ; i.e., if $B_x < \infty$ implies $B_y < \infty$, where

$$B_x \triangleq \bigvee_{t \in \text{Spt}(x)} |x(t)|. \quad (6)$$

The morphological *zero impulse*

$$\mu(t) \triangleq \begin{cases} 0, & t = 0, \\ -\infty, & t \neq 0, \end{cases} \quad (7)$$

is an elementary signal useful for analyzing morphological systems. For example, any signal can be represented as a supremum of translated impulses:

$$x(t) = \bigvee_{\tau=-\infty}^{\infty} x(\tau) + \mu(t - \tau). \quad (8)$$

Further, the output of a DTI system \mathcal{D} when the input is the impulse, henceforth defined as its *impulse response*

$$g(t) \triangleq \mathcal{D}[\mu(t)], \quad (9)$$

uniquely characterizes a DTI system in the time domain and determines its causality and stability, as shown next.

Theorem 1. A system \mathcal{D} with $g = \mathcal{D}(\mu)$ is

- (a) DTI iff $\mathcal{D}(x) = x \oplus g$.
- (b) Causal iff $g(t) = -\infty \quad \forall t < 0$.
- (c) Anti-Causal iff $g(t) = -\infty \quad \forall t > 0$.
- (d) Stable iff $\sup \{|g(t)|: t \in \text{Spt}(g)\} < \infty$.

Proof. (a) If \mathcal{D} is a morphological dilation by g as in (1), then it is a DTI system. The converse follows from (5) and (8). (b) and (c) follow from the definitions of causality since the output can be written as $\mathcal{D}(x)(t) = \bigvee_{\tau} x(t - \tau) + g(\tau)$. (d) Sufficiency: If x and g have finite bounds B_x and B_g within their supports, then their dilation $y = x \oplus g$ is also bounded because $|y(t)| \leq B_x + B_g$ for all $t \in \text{Spt}(x) \oplus \text{Spt}(g)$. Necessity: Assume now that \mathcal{D} is stable. Then B_g must be finite, because otherwise we can find a bounded input yielding an unbounded output. For example, the input $x(t) = \mu(t)$ yields as output $y(t) = g(t)$. Obviously, x is bounded. Thus, if $B_g = \infty$ we get an unbounded output. \square

Thus, any DTI system is equivalent to a morphological dilation by its impulse response. Further, it is causal if and only if (in short, iff) its impulse response is right-sided, and stable iff the max absolute value of its impulse response (over its support) is finite.

3. Slope transforms

The lines, i.e., affine signals $x(t) = \alpha t + b$ are *eigenfunctions* of any DTI system \mathcal{D} because the corresponding outputs are

$$\mathcal{D}[\alpha t + b] = \alpha t + b + G(\alpha), \quad (10)$$

where the corresponding eigenvalue is

$$G(\alpha) = \bigvee_t g(t) - \alpha t. \quad (11)$$

We call $G(\alpha)$ the *slope response* of the DTI system. It measures the amount of shift in the intercept of the input lines with slope α . It is also conceptually similar to the frequency response of LTI systems which is their multiplicative eigenvalue for input exponentials, whereas G is the additive eigenvalue of DTI systems for input lines. In addition, viewing

$G(\alpha)$ as a transform for the signal $g(t)$ with variable the slope α leads us to the development of slope transforms for arbitrary signals.

3.1. Continuous-time signals

To acquire a geometrical intuition behind the slope transforms we precede their definitions with a brief summary of concepts from the closely-related Legendre transform and some definitions of concave and convex signals for which the analysis of slope transforms is simple.

Given a real-valued function f whose domain is a subset of \mathbb{R} , f is *concave* iff

$$f(t) \geq \frac{pf(t-q) + qf(t+p)}{p+q} \quad \forall p, q > 0 \text{ and } \forall t. \quad (12)$$

For equivalent definitions, see [19]. If its domain is smaller than \mathbb{R} , the function f can be viewed as concave over all \mathbb{R} by allowing it to have $-\infty$ values at all points where it was originally undefined [19]. A function f is *convex* if $-f$ is concave, i.e., if the \geq in (12) is replaced by \leq .

Let a signal $x(t)$ be concave and have an invertible derivative $x' = dx/dt$. At each point $(t, x(t))$ on the signal's graph the *tangent* line has *slope* $\alpha = x'(t)$ and *intercept* equal to

$$X = x(t) - \alpha t. \quad (13)$$

Eliminating t from (13) yields

$$X(\alpha) = x((x')^{-1}(\alpha)) - \alpha[(x')^{-1}(\alpha)], \quad (14)$$

where f^{-1} denotes the inverse of a function f . The tangent's intercept X , as a function of the slope, is the Legendre transform [2] of the signal x .

The relation $x = x(t)$ can also be recovered from $X = X(\alpha)$ as an inverse Legendre transform. This is based on viewing the graph of x as the lower envelope of all its tangent lines. Thus, by (13) we have $X'(\alpha) = -t$; using this to eliminate α from (13) yields

$$x(t) = X((X')^{-1}(-t)) + t[(X')^{-1}(-t)]. \quad (15)$$

The right-hand side is the inverse Legendre transform of X .

If the signal x is convex, then similar ideas apply where the signal is viewed as the upper envelope of its tangent lines.

If the signal derivative is not invertible, or the signal is not everywhere differentiable, or if the signal is neither convex nor concave, there are more general transforms discussed next.

3.1.1. Slope transforms based on supremum and infimum

Viewing the slope response (11) as a signal transform with variable the slope α , Maragos [8] was motivated to define for any signal $x: \mathbb{R} \rightarrow \bar{\mathbb{R}}$ its *upper slope transform* as the function $X_\vee: \mathbb{R} \rightarrow \bar{\mathbb{R}}$ with

$$X_\vee(\alpha) \triangleq \bigvee_{t \in \mathbb{R}} x(t) - \alpha t, \quad \alpha \in \mathbb{R}. \quad (16)$$

The mapping between the signal and its transform is denoted by $\mathcal{A}_\vee: x(t) \mapsto X_\vee(\alpha)$.

As discussed later, the signals $\alpha t + b$ are also eigenfunctions of erosion translation-invariant systems. The corresponding eigenvalue is given by another slope transform based on infimum. Specifically, for any signal $x: \mathbb{R} \rightarrow \bar{\mathbb{R}}$ its *lower slope transform* is defined in [8] as the function $X_\wedge: \mathbb{R} \rightarrow \bar{\mathbb{R}}$ with

$$X_\wedge(\alpha) \triangleq \bigwedge_{t \in \mathbb{R}} x(t) - \alpha t, \quad \alpha \in \mathbb{R}. \quad (17)$$

Obviously,

$$X_\wedge(\alpha) \leq X_\vee(\alpha) \quad \forall \alpha. \quad (18)$$

Denoting the mapping between the signal and its lower slope transform¹ by $\mathcal{A}_\wedge: x(t) \mapsto X_\wedge(\alpha)$, we easily find a relationship between the two slope transforms:

$$\begin{aligned} \mathcal{A}_\wedge[x(t)](\alpha) &= -\mathcal{A}_\vee[-x(t)](-\alpha) \\ &= -\mathcal{A}_\vee[-x(-t)](\alpha). \end{aligned} \quad (19)$$

The above definition of slope transforms was entirely motivated by the form of the eigenfunctions and eigenvalues of DTI and ETI systems.

¹In convex analysis [19], given a convex function f there corresponds another convex function $f^*(\alpha) \triangleq \bigvee_t \alpha t - f(t)$ called the *conjugate* of f . The correspondence between f and f^* is one-to-one because $f(t) = \bigvee_\alpha \alpha t - f^*(\alpha)$. The lower slope transform of f and its conjugate function are closely related since $f^*(\alpha) = -F_\wedge(\alpha)$.

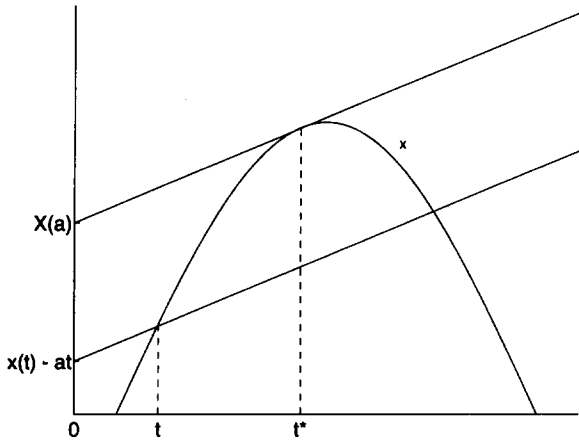


Fig. 1. Concave signal x , its tangent with slope α , and a line parallel to the tangent.

However, there is also a close relationship with the Legendre transform. To see this, assume that the signal $x(t)$ is concave and has an invertible derivative. The intercept of a line that passes from the point $(t, x(t))$ on the signal's graph and has slope α is equal to $x(t) - \alpha t$; see Fig. 1. For a fixed α , as t varies there is a time instant t^* for which the intercept attains its maximum value. This occurs when the line becomes tangent to the graph; then we have $x'(t^*) = \alpha$. As α varies, this maximum intercept becomes a function of the slope α and is equal to the upper slope transform (by the latter's definition). Further, the maximization of the con-

cave intercept function $x(t) - \alpha t$ can be found exactly from its value at its unique stationary point t^* where $x'(t^*) = \alpha$. Thus, if the signal x is concave and has an invertible derivative, then the upper slope transform is equal to its Legendre transform, with a possible exception due to boundary effects [9]. For such an example (see also Fig. 2) consider the concave cosine pulse

$$y(t) = \cos(\omega_0 t), \quad |t| \leq T/4, \tag{20}$$

where $T = 2\pi/\omega_0$. Then $y'(t) = -\omega_0 \sin(\omega_0 t)$ and the maximum intercept occurs at $t^* = -\arcsin(\alpha/\omega_0)/\omega_0$, where $|\alpha| \leq \omega_0$, and $|\arcsin(\cdot)| \leq \pi/2$. Thus,

$$Y_v(\alpha) = \sqrt{1 - \frac{\alpha^2}{\omega_0^2}} + \left(\frac{\alpha}{\omega_0}\right) \arcsin\left(\frac{\alpha}{\omega_0}\right). \tag{21}$$

Similarly, if a signal is convex and has an invertible derivative, its lower slope transform is equal to its Legendre transform.

Now if the signal is concave or convex but either (i) it does not have an invertible derivative, e.g., when its graph contains some line segments or (ii) it is not differentiable everywhere on its support, i.e., when it has some corner points, then its Legendre transform cannot be found analytically via stationary points but the slope transforms still give an answer. An important example of case (i) is a signal $f(t) = \alpha_0 t$. Then f' is not invertible, but the maximization of the intercept becomes simple

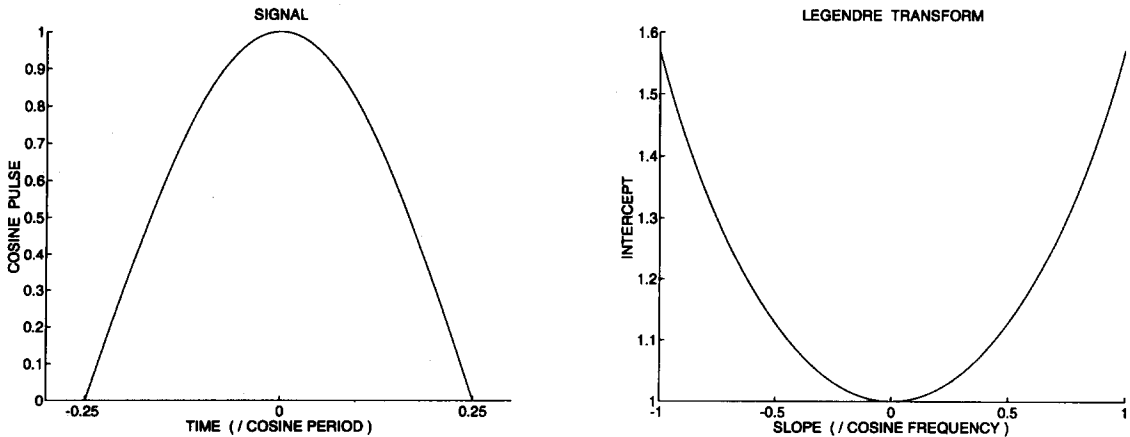


Fig. 2. Concave cosine pulse and its upper slope transform (equal to the Legendre transform).

if we express it via the supremum in (16). Thus, $F_{\vee}(\alpha) = \bigvee_t(\alpha_0 - \alpha)t$. Similarly, $F_{\wedge}(\alpha) = \bigwedge_t(\alpha_0 - \alpha)t$. Thus,

$$\alpha_0 t \xleftrightarrow{\mathcal{A}_{\vee}} -\mu(\alpha - \alpha_0), \quad (22)$$

$$\alpha_0 t \xleftrightarrow{\mathcal{A}_{\wedge}} \mu(\alpha - \alpha_0). \quad (23)$$

Thus, the slope transforms of a morphological system's eigenfunction $\alpha_0 t$ are impulses at slope α_0 .

If the signal is neither concave nor convex, then its Legendre transform is not a single-valued function. In this case the upper (respectively lower) slope transform still provides a single-valued function, which is the slope transform of the smallest upper concave (respectively greatest lower convex) envelope of the signal, as shown next. In general,

$$X_{\wedge}(\alpha) + \alpha t \leq x(t) \leq X_{\vee}(\alpha) + \alpha t, \quad \forall \alpha, \forall t. \quad (24)$$

Thus, $x(t)$ is covered from above by all the lines $X_{\vee}(\alpha) + \alpha t$ whose infimum creates the upper signal envelope

$$\hat{x}(t) \triangleq \bigwedge_{\alpha \in \mathbb{R}} X_{\vee}(\alpha) + \alpha t. \quad (25)$$

Likewise, $x(t)$ is covered from below by all the lines $X_{\wedge}(\alpha) + \alpha t$ whose supremum creates the lower envelope

$$\check{x}(t) \triangleq \bigvee_{\alpha \in \mathbb{R}} X_{\wedge}(\alpha) + \alpha t. \quad (26)$$

Thus, if we view the mapping $\mathcal{A}_{\vee}^{-1}: X_{\vee} \mapsto \hat{x}$ as an 'inverse' upper slope transform and the mapping $\mathcal{A}_{\wedge}^{-1}: X_{\wedge} \mapsto \check{x}$ as an 'inverse' lower slope transform, the following theorem states several important properties of the slope transforms and their inverses. Its proof is in [9].

Theorem 2 (Maragos [9]). *For any signal $x: \mathbb{R} \rightarrow \overline{\mathbb{R}}$,*

- (a) $X_{\vee}(\alpha)$ and $\check{x}(t)$ are convex, whereas $X_{\wedge}(\alpha)$ and $\hat{x}(t)$ are concave.
- (b) For all t , $\check{x}(t) \leq x(t) \leq \hat{x}(t)$.
- (c) At any time instant t

$$\hat{x}(t) = x(t) \Leftrightarrow$$

$$x(t) \geq \frac{px(t-q) + qx(t+p)}{p+q} \quad \forall p, q > 0. \quad (27)$$

At any t , $x(t) = \check{x}(t)$ iff the \geq sign in (27) is replaced by \leq .

- (d) $\hat{x}(t) = x(t)$ for all t if x is concave, and $\check{x} = x$ if x is convex.
- (e) \hat{x} is the smallest concave upper envelope of x , and \check{x} is the greatest convex lower envelope of x .

Thus, there is one-to-one correspondence between $X_{\vee}(\alpha)$ and the signal envelope $\hat{x}(t)$. However, all signals between $x(t)$ and $\hat{x}(t)$ will have the same upper slope transform:

$$x(t) \leq y(t) \leq \hat{x}(t) \quad \forall t \Rightarrow X_{\vee}(x) = Y_{\vee}(x). \quad (28)$$

If a signal x is concave and has an invertible derivative, then its inverse Legendre transform and the inverse upper slope transform become equal. Namely, since x is the lower envelope of its tangent lines, for each t $x(t)$ is the minimum value of $X(\alpha) + \alpha t$, which leads us to the inverse upper slope transform. Alternatively, the minimization over α of the convex function $X(\alpha) + \alpha t$ can be done by finding its value at the stationary point $\alpha^* = (X')^{-1}(-t)$, which leads to the inverse Legendre transform. However, if X is not differentiable, then we can directly use only the inverse upper slope transform. Such a case is the slope transform (22) of a line, where the inverse upper slope transform yields the answer in a simple way: $\bigwedge_{\alpha} \alpha t - \mu(\alpha - \alpha_0) = \alpha_0 t$.

Table 1 lists several properties of the upper slope transform. Next we prove Property 8 which is the most important. The proofs of the rest can be found in [9].

$$\begin{aligned} \mathcal{A}_{\vee}[x(t) \oplus y(t)](\alpha) &= \bigvee_t \left(\bigvee_{\tau} x(\tau) + y(t - \tau) \right) - \alpha t \\ &= \bigvee_{\tau} x(\tau) + \left(\bigvee_t y(t - \tau) - \alpha t \right) \\ &= \bigvee_{\tau} x(\tau) + Y(\alpha) - \alpha \tau \\ &= X(\alpha) + Y(\alpha). \end{aligned} \quad (29)$$

Thus, dilation in the time domain corresponds to addition in the slope domain. Note the analogy with LTI systems where convolving two signals in time corresponds to multiplying their Fourier transforms. If two signals are concave, then their

Table 1
Properties of upper slope transform

| No. | Signal: $x(t)$ | Transform: $X(\alpha) = \bigvee_t x(t) - \alpha t$ |
|-----|-----------------------------------------------------------------------------|-------------------------------------------------------|
| 1. | $\bigvee_i c_i + x_i(t)$ | $\bigvee_i c_i + X_i(\alpha)$ |
| 2. | $x(t - t_0)$ | $X(\alpha) - \alpha t_0$ |
| 3. | $x(t) + \alpha_0 t$ | $X(\alpha - \alpha_0)$ |
| 4. | $x(rt)$ | $X(\alpha/r)$ |
| 5. | $x(-t)$ | $X(-\alpha)$ |
| 6. | $x(t) = x(-t)$ | $X(\alpha) = X(-\alpha)$ |
| 7. | $rx(t), r > 0$ | $rX(\alpha/r)$ |
| 8. | $x(t) \oplus y(t)$ | $X(\alpha) + Y(\alpha)$ |
| 9. | $\bigvee_t x(\tau) + y(t + \tau)$ | $X(-\alpha) + Y(\alpha)$ |
| 10. | $x(t) \leq y(t) \quad \forall t$ | $X(\alpha) \leq Y(\alpha) \quad \forall \alpha$ |
| 11. | $x(t) \leq X(0) \quad \forall t$ | $X(\alpha) \geq x(0) \quad \forall \alpha$ |
| 12. | $x(t) \wedge y(t)$ | $\leq X(\alpha) \wedge Y(\alpha)$ |
| 13. | $x(t) + y(t)$ | $\leq \bigwedge_b X(b) + Y(\alpha - b)$ |
| 14. | $y(t) = \begin{cases} x(t), & t \leq T \\ -\infty, & t > T \end{cases}$ | $Y(\alpha) = X(\alpha) \ominus (-T \alpha)$ |
| 15. | $x(t) + y(t), \text{ convex } y$ | $X_{\vee}(\alpha) \oplus Y_{\wedge}(\alpha)$ |

Table 2
Examples of upper slope transforms

| No. | Signal: $x(t)$ | Transform: $X(\alpha) = \bigvee_t x(t) - \alpha t$ |
|-----|--------------------------------------------------------------------------|------------------------------------------------------------------------------------------------------|
| 1. | $\alpha_0 t + s(t)$ | $-s(\alpha - \alpha_0)$ |
| 2. | $\alpha_0 t + s(-t)$ | $-s(\alpha_0 - \alpha)$ |
| 3. | $\mu(t - t_0)$ | $-\alpha t_0$ |
| 4. | $s(t - t_0)$ | $-\alpha t_0 - s(\alpha)$ |
| 5. | $x(t) = \begin{cases} 0, & t \leq T \\ -\infty, & t > T \end{cases}$ | $X(\alpha) = T \alpha $ |
| 6. | $x(t) = -\alpha_0 t , \alpha_0 > 0$ | $X(\alpha) = \begin{cases} 0, & \alpha \leq \alpha_0 \\ \infty, & \alpha > \alpha_0 \end{cases}$ |
| 7. | $\sqrt{1 - t^2}, t \leq 1$ | $\sqrt{1 + \alpha^2}$ |
| 8. | $-t^2/2$ | $\alpha^2/2$ |
| 9. | $- t ^p/p, p > 1$ | $ \alpha ^q/q, 1/p + 1/q = 1$ |
| 10. | $\exp(t)$ | $\alpha[1 - \log(\alpha)]$ |
| 11. | $\tanh(t), t \geq 0$ | $\sqrt{1 - \alpha} - \alpha \log\left(\frac{1 + \sqrt{1 - \alpha}}{\sqrt{\alpha}}\right)$ |
| 12. | $-t \log(t) - (1 - t) \times \log(1 - t), 0 \leq t \leq 1$ | $\log[1 + \exp(\alpha)] - \alpha$ |

dilation can be done by first transforming the signals to the slope domain, adding their upper slope transforms, and then applying an inverse upper slope transform to return to the time domain. This opens new ways of implementing dilations, since addition is a much simpler operation.

Whatever we discussed for upper slope transforms also applies to the lower slope transform, the only differences being the interchange of suprema with infima, concave with convex, and dilation with erosion.

Table 2 contains several examples of slope transforms. (For proofs see [9].) We know that the upper slope transform of a line $\alpha_0 t$ is a negated impulse at slope α_0 . Adding to it the morphological *zero step*

$$s(t) \triangleq \begin{cases} 0, & t \geq 0, \\ -\infty, & t < 0 \end{cases} \quad (30)$$

makes it a right-sided signal $\alpha_0 t + s(t)$ (also called 'causal', in analogy to the impulse response of causal DTI systems), whose upper slope transform is a negated step at slope α_0 . Likewise, the left-sided semi-infinite line $\alpha_0 t + s(-t)$ transforms into a step in the slope domain. There is a duality between the time and slope domain, similar to the duality between time and frequency domains of Fourier transform pairs. Thus Examples 3 and 4 state that the slope transform of a time impulse or step is an infinite or semi-infinite line, respectively. Further (see Examples 5 and 6), a rectangular time pulse becomes a cone in the slope domain, whereas a time cone transforms into a slope pulse which (viewed as a system's slope response) only passes a finite zone of slopes.

Consider the rectangular time pulse $w(t)$, equal to 0 for $t \leq -T$ and $-\infty$ else, added to a signal $x(t)$. This acts as a time-limiter (or rectangular time windowing) for x . By Property 14 in Table 1, the upper slope transform of the time-limited signal $x(t) + w(t)$ is the erosion of the original signal's slope transform $X(\alpha)$ by the negative of the window's slope transform $W(\alpha) = T|\alpha|$. The result [9] of this conical erosion will be to replace high-slope parts of the original transform X with lines of slope $\pm T$. This is a kind of nonlinear blurring. Consider the analogy with the blurring that occurs when we multiply a signal x by a time window in which case

the original Fourier transform of x is convolved with the window's Fourier transform.

Examples 7-12 deal with functions x with invertible derivatives. Hence we can find their slope transforms using stationary point values $x(t^*) - \alpha t^*$, where $x'(t^*) = \alpha$. Thus, a concave time parabola becomes a convex parabola in the slope domain [6]. As observed in [4], the parabola plays the same role in slope transforms as the Gaussian function does for Fourier transforms: the transform belongs to the same class of functions as the signal. This parabola transform pair is actually a special case of a general class (Example 9) of convex-conjugate function pairs [19].

3.1.2. Duality between the upper and lower slope transform

Consider the complete lattice \mathcal{L} of all signals $f: E \rightarrow \mathbb{R}$ equipped with the \vee, \wedge operations. Then the upper slope transform mapping $\mathcal{A}_\vee: \mathcal{L} \rightarrow \mathcal{L}$ and its inverse \mathcal{A}_\vee^{-1} are signal operators on \mathcal{L} that are a lattice dilation and erosion, respectively, since they distribute over supremum and infimum. Further, for any signal $f \in \mathcal{L}$, Theorem 2 states that $f \leq \hat{f}$, or equivalently

$$f \leq \mathcal{A}_\vee^{-1}(\mathcal{A}_\vee(f)). \tag{31}$$

The inverse upper slope transform mapping is closely related to the forward lower slope transform mapping \mathcal{A}_\wedge since $\mathcal{A}_\wedge = \mathcal{R}\mathcal{A}_\vee^{-1} = \mathcal{A}_\vee^{-1}\mathcal{R}$, where $\mathcal{R}: f(t) \mapsto f(-t)$ is the reflection operator. Likewise, $\mathcal{A}_\wedge^{-1} = \mathcal{A}_\vee\mathcal{R}$. Hence, $f = \mathcal{A}_\wedge^{-1}\mathcal{A}_\wedge(f) = \mathcal{A}_\vee\mathcal{A}_\vee^{-1}(f)$ since \mathcal{R}^2 is the identity operator. Thus, for any signal f ,

$$\mathcal{A}_\vee(\mathcal{A}_\vee^{-1}(f)) \leq f. \tag{32}$$

The two above results imply that $(\mathcal{A}_\vee^{-1}, \mathcal{A}_\vee)$ form an adjunction² [5], also called a morphological duality pair [17]. Consequently, the mapping $\mathcal{A}_\vee^{-1}\mathcal{A}_\vee: f \mapsto \hat{f}$ is a lattice closing, i.e., increasing ($f \leq g \Rightarrow \hat{f} \leq \hat{g}$), extensive ($f \leq \hat{f}$) and idempotent ($\hat{\hat{f}} = \hat{f}$).

²The idea that the upper and lower slope transforms might be related via an adjunction was suggested to me by Heijmans in a discussion in May 1993.

Likewise, $(\mathcal{A}_\wedge, \mathcal{A}_\wedge^{-1})$ is also an adjunction, and the mapping $\mathcal{A}_\wedge^{-1}\mathcal{A}_\wedge: f \mapsto \check{f}$ is a lattice opening, i.e., increasing, anti-extensive ($\check{f} \leq f$) and idempotent.

3.1.3. Slope transform based on stationary points

For differentiable signals x , a more general expression for their Legendre transform (14) used in [4] is

$$X_{\text{stat}}(\alpha) \triangleq \text{stat}_t\{x(t) - \alpha t\} = \{x(t) - \alpha t: x'(t) = \alpha\}, \tag{33}$$

where $\text{stat}_t\{f(t)\} \triangleq \{f(t): f'(t) = 0\}$. Thus, for each α , $X_{\text{stat}}(\alpha)$ is a set of numbers since the equation $x'(t) = \alpha$ might have more than one solutions. If x' is invertible, then X_{stat} is a single-valued function identical to the Legendre transform. If x is neither convex nor concave, then X_{stat} is a multi-valued function, i.e., a set collection of single-valued transform functions. It is this multivalued Legendre transform that Dorst and Van den Boomgaard defined in [4] as a slope transform for differentiable signals. The inverse transform reconstructs the signal from the set collection of transform functions:

$$x(t) = \text{stat}_\alpha\{X_{\text{stat}}(\alpha) + \alpha t\}, \tag{34}$$

where for each α the operation $X_{\text{stat}}(\alpha) + \alpha t$ is meant as adding to all the members of the set $X_{\text{stat}}(\alpha)$ the number αt .

For example, consider the cosine over all time:

$$x(t) = \cos(\omega_0 t), \quad t \in \mathbb{R}, \tag{35}$$

which is an infinite sequence of convex and concave half-period cosine pulses. Then its multivalued Legendre transform consists of an infinite number of different functions, one for each convex or concave piece:

$$X_{\text{stat}}(\alpha) = \{Y_\vee(\alpha) + \alpha kT, -Y_\vee(\alpha) + \alpha T(k - 0.5): k = 0, \pm 1, \pm 2, \dots\}, \tag{36}$$

where Y_\vee is the slope transform (21) of a single concave cosine pulse. Fig. 3 shows four of these transform functions. In general, the number of different functions in the multivalued Legendre transform is equal to the number of consecutive convex and concave pieces making up the signal. This could be finite or infinite. When we use the inverse

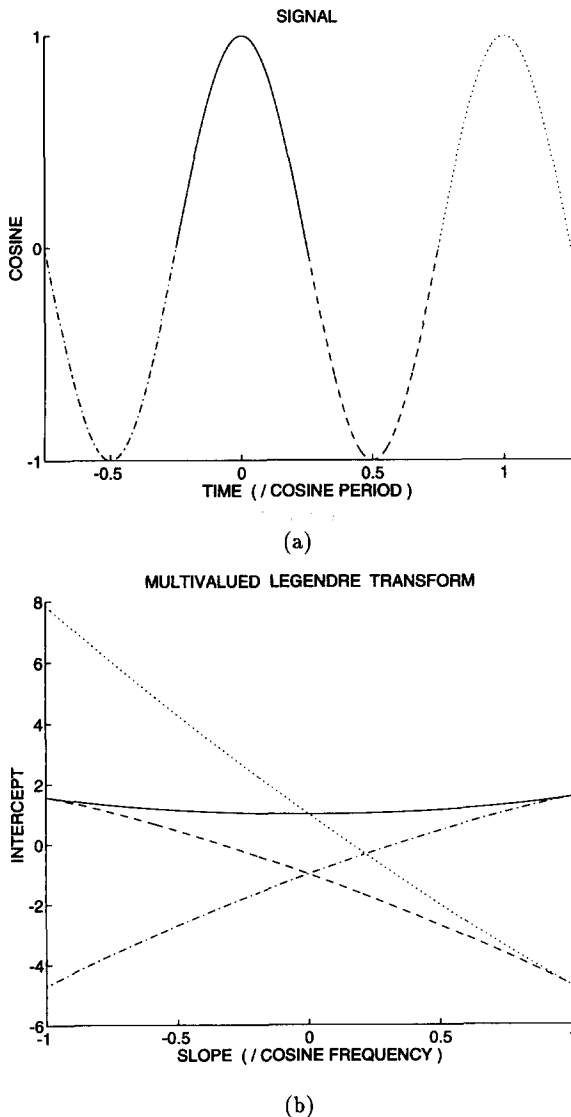


Fig. 3. (a) Two periods of a cosine and (b) the upper or lower slope transforms (equal to Legendre transforms) of the four concave or convex cosine pulses. (The line type of each time pulse is the same with the line type of its transform.)

of the multivalued Legendre transform, then minimization of each individual function in $X_{\text{stat}}(\alpha) + \alpha t$ over α will reconstruct the original signal only over the time interval over which the corresponding convex or concave piece is defined.

In [4] several properties of the multivalued Legendre transform were given which seem similar to the properties of the upper/lower slope transform, but there are some important differences. First, the multivalued Legendre transform is set-valued, and hence adding lines to, or shifting and scaling of this transform has to be understood as a simultaneous vector translation or homothetic scaling of a set. Second, and most important, the dilation–addition property (29) of the upper slope transform must undergo two significant changes in order to retain a similar form for the multivalued Legendre transform: the supremum in the morphological signal dilation (1) is replaced by values at stationary points (and hence it becomes set-valued), and the addition of transforms becomes a Minkowski set addition.

In general, an arbitrary signal can be analyzed using slope transforms in at least two different ways corresponding to two different goals: signal reconstruction, or envelope reconstruction. If the goal is exact signal reconstruction, then we should first segment the signal into consecutive convex and concave pieces. If the signal x is twice differentiable, this can be done by finding the inflection points $x'' = 0$, where we have transitions between convexity and concavity. Then we find the slope transform of each piece, either using stationary points if it is a known and differentiable mathematical function, or using the sup/inf-based slope transforms for general signals. The result will generally be a set collection of slope transforms of the signal pieces, which can reconstruct the signal exactly. The disadvantage here is the multivaluedness of the transform. Alternatively, if the analysis goal is to extract information about the long-time behavior of the signal, as manifested by its upper and lower envelope, then we should compute its upper and lower slope transforms and take their inverses, which give us the two envelopes. For example, if the signal is the impulse response of a recursive DTI system (discussed later) or if it is an amplitude-modulated signal, then its short-time oscillations may not be important. In this case, the composition of forward and inverse upper or lower slope transform captures only its important (for the specific application) long-time structure, i.e., its upper or lower envelope.

3.2. Slope transforms for discrete-time signals

Consider sampling a continuous-time signal $x_c(t)$ at time instants $t = nT$, where $n \in \mathbb{Z}$ is the integer time index and T is the sampling period. For applying slope transforms, the sampling can be modeled as addition of the original signal with a periodic (morphological) impulse train

$$p(t) = \bigvee_{n=-\infty}^{\infty} \mu(t - nT). \quad (37)$$

Thus the sampled continuous-time signal is

$$x_s(t) = x_c(t) + p(t) = \bigvee_n x[n] + \mu(t - nT), \quad (38)$$

where $x[n] = x_c(nT)$ is the discrete-time signal. If $X_c(\alpha)$ denotes the upper slope transform of $x_c(t)$, then the upper slope transform of $x_s(t)$ is

$$X_s(\alpha) = \bigvee_n x[n] - \alpha nT \leq X_c(\alpha). \quad (39)$$

The inequality results because the supremum in X_s is taken only over the discrete time instants. Now if we define the upper slope transform of the discrete-time signal $x[n]$ by

$$X_v(\alpha) \triangleq \bigvee_{n=-\infty}^{\infty} x[n] - \alpha n, \quad \alpha \in \mathbb{R}, \quad (40)$$

we have that

$$X_v(\alpha) = X_s(\alpha/T) \leq X_c(\alpha/T). \quad (41)$$

Namely, the upper slope transform of the discrete-time signal is a slope-scaled version of the transform of the continuous-time sampled signal and smaller or equal to the slope-scaled version of the transform of the original continuous-time signal. Another effect of sampling, as shown in Fig. 4, is to replace parts of the slope transform of the continuous-time signal with supporting lines.

Henceforth, whenever we deal with discrete-time signals we shall not be concerned with whether they originated from sampling a continuous-time signal or they are inherently discrete. Further, we also define the lower slope transform of any discrete-time signal $x: \mathbb{Z} \rightarrow \mathbb{R}$ as the function

$$X_\wedge(\alpha) \triangleq \bigwedge_{n=-\infty}^{\infty} x[n] - \alpha n, \quad \alpha \in \mathbb{R}. \quad (42)$$

The definitions of inverse upper and lower slope transforms are identical to the continuous-time case, except that the time variable is discrete. Theorem 2 and the properties of the upper and lower envelopes obtained via the inverse slope transforms also hold in discrete time. The definitions of

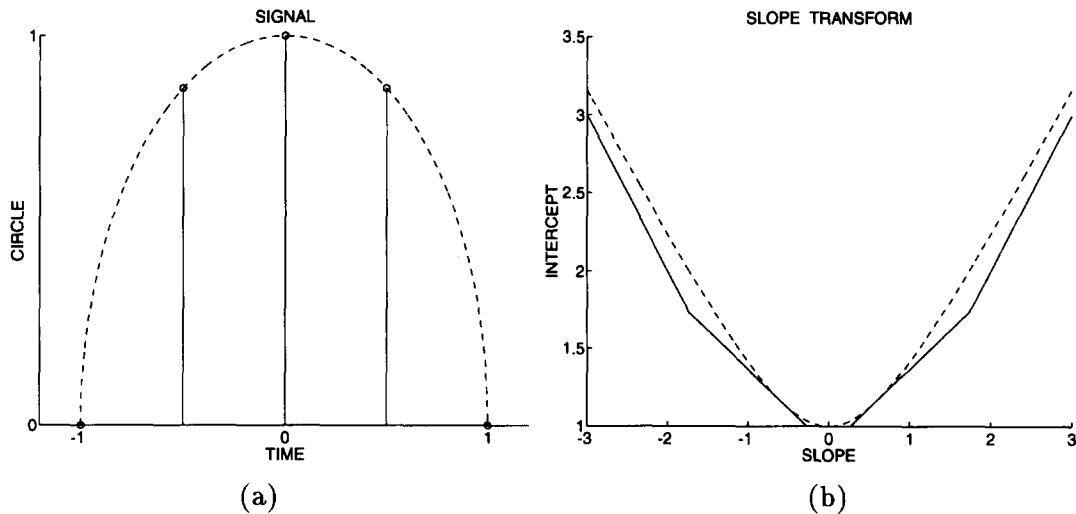


Fig. 4. (a) Signal circle (in dashed line) $x_c(t) = \sqrt{1 - t^2}$, $|t| \leq 1$, and its sampled version (in solid lines $x_s(t) = x_c(nT)$ with $T = 0.5$). (b) Upper slope transforms of original circle (in dashed line) and of its sampled version (in solid line).

convexity and concavity remain the same as (12), but all the time variables are integers. Likewise, the properties of the discrete-time slope transforms are identical to all their continuous-time counterparts in Table 1, except for Property 4 which does not hold in discrete time.

Examples 1-6 of slope transform pairs in Table 2 also hold in discrete time in identical form, except that the time variables and constants must be discrete. For example, the discrete-time pulse defined as $x[n] = 0$ for $|n| \leq N$ and $-\infty$ else, has slope transform $X_v(\alpha) = N|\alpha|$ and $x = \hat{x}$. Further, as an example illustrative of (28), let $y[n] = 0$ for $n = \pm N$ and $-\infty$ else. Then $Y_v(\alpha) = X_v(\alpha)$ and $\hat{y}[n] = y[n]$ for $|n| \geq N$, but $\hat{y}[n] > y[n]$ for $|n| < N$.

Examples 7-12 in Table 2, whose slope transform was found via stationary points, may not have the same form in discrete time because the derivative-based methods to find maxima/minima of functions do not apply. For instance, consider the discrete-time parabola

$$x[n] = -n^2/2. \tag{43}$$

Then, for each α , the maximum value of $x[n] - \alpha n$ occurs at one of the two integers closest to $-\alpha$. This yields

$$X_v(\alpha) = - \left((0.5 \lfloor -\alpha \rfloor^2 + \alpha \lfloor -\alpha \rfloor) \wedge (0.5 \lceil -\alpha \rceil^2 + \alpha \lceil -\alpha \rceil) \right). \tag{44}$$

Fortunately, in discrete-time the computation of the upper slope transform for a *finite-length* signal $x[n], n = 0, 1, \dots, N-1$, is very simple. It is equal to $X_v(\alpha) = \max\{x[n] - \alpha n: 0 \leq n \leq N-1\}$. Thus, for each slope value α , it requires N additions and multiplications and $N-1$ comparisons; hence it has linear complexity. In contrast, the slope transform based on stationary points (i.e., the single- or multi-valued Legendre transform) cannot generally be computed in discrete time unless some approximation is done for derivatives.

As a numerical example of discrete slope transforms consider two finite-length signals and their dilation:

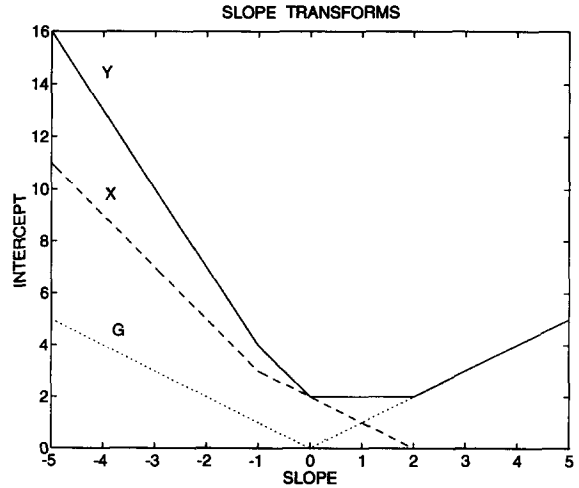


Fig. 5. Discrete-time upper slope transforms $X(\alpha)$, $G(\alpha)$ and $Y(\alpha) = X(\alpha) + G(\alpha)$ of the signals $x[n] = 0, 2, 1$ for $n = 0, 1, 2$, $g[n] = 0$ for $n = -1, 0, 1$, and $y[n] = x \oplus g[n]$.

$$\begin{array}{cccccccc} n & = & -2 & -1 & 0 & 1 & 2 & 3 & 4 \\ x[n] & = & - & - & 0 & 2 & 1 & - & - \\ g[n] & = & - & 0 & 0 & 0 & - & - & - \\ x[n] \oplus g[n] = y[n] & = & - & 0 & 2 & 2 & 2 & 1 & - \end{array}$$

where $-$ denotes $-\infty$. The corresponding upper slope transforms (shown in Fig. 5) are

$$X(\alpha) = \max[0, 2 - \alpha, 1 - 2\alpha],$$

$$G(\alpha) = |\alpha|,$$

$$X(\alpha) + G(\alpha) = Y(\alpha) = \max[\alpha, 2, 2 - 2\alpha, 1 - 3\alpha].$$

4. Max difference equations

A very large class of discrete LTI systems [14, 13] can be described via the following linear difference equations:

$$y[n] = \sum_{k=1}^N a_k y[n-k] + \sum_{m=1}^M b_m x[n-m], \tag{45}$$

where x is the input and y is the output signal. Replacing sum with maximum and multiplication

with addition gives us the following nonlinear max difference equation:

$$y[n] = \left(\bigvee_{k=1}^N a_k + y[n-k] \right) \vee \left(\bigvee_{m=0}^M b_m + x[n-m] \right) \quad (46)$$

capable of describing all discrete-time morphological dilations with structuring elements of finite or infinite length. All signals in this section are defined on \mathbb{Z} . The signal values and all coefficients a_k, b_m are from $\mathbb{R} \cup \{-\infty\}$. If some $a_k = -\infty$, the term with $y[n-k]$ is not used in the equation. N is the order of the equation, assuming $a_N > -\infty$.

Viewing (46) as a nonlinear system $\Psi: x \mapsto y = \Psi(x)$, we need the following concepts for its analysis. To solve (46) in forward time $n \geq n_0$ we need N initial conditions $IC[n_0]$, where

$$IC[n] \triangleq \{y[n-1], y[n-2], \dots, y[n-N]\}.$$

If all the values in $IC[n_0]$ are $-\infty$, the initial state of the system does not affect its output. We define the impulse response g of Ψ as its output when the input is the impulse and $IC[0] = -\infty$. Finally, to analyze (46) we also need two basic signals: the discrete-time zero impulse $\mu[n]$ and step $s[n]$, which are defined identically to their continuous-time counterparts.

Consider the first-order max difference equation, with $a, b \in \mathbb{R}$,

$$y[n] = \max(y[n-1] + a, x[n] + b). \quad (47)$$

By induction on $n \geq 0$ we can find its solution:

$$y[0] = (b + x[0]) \vee (a + y[-1]), \quad (48)$$

$$y[1] = (b + (x[1] \vee (x[0] + a))) \vee (2a + y[-1]), \quad (49)$$

\vdots

$$y[n] = \underbrace{\left(b + \bigvee_{k=0}^n x[k] + (n-k)a \right)}_{= x[n] \oplus g[n]} \vee (a(n+1) + y[-1]), \quad (50)$$

where $g[n]$ is the impulse response equal to

$$g[n] = an + b + s[n] = \begin{cases} an + b, & n \geq 0, \\ -\infty, & n < 0. \end{cases} \quad (51)$$

Thus the general solution $y[n]$ of (47) is the maximum of the $(-\infty)$ -state response (i.e., the dilation $x \oplus g$) and the $(-\infty)$ -input response due only to the initial condition $y[-1]$. The system is stable only if $a = 0$. Similar results are also true for the general N th-order max difference equation.

Initial conditions $\neq -\infty$ could be useful in some applications; e.g., if $y[-1] > -\infty$, the solution of (47) is constrained to be $\geq a(n+1) + y[-1]$. However, in the rest of the paper we shall assume $-\infty$ initial conditions.

Theorem 3. *The max difference equation (46) corresponds to a causal DTI system if (i) whenever $x[n] = -\infty$ for all $n < n_0$ then $y[n] = -\infty$ for all $n < n_0$, where n_0 is an arbitrary but otherwise fixed time instant, and (ii) the required initial conditions $IC[n_0]$ are $-\infty$.*

Proof. It is similar to the proof in [14] that the linear difference equation (45) is equivalent to a causal LTI system if whenever $x[n] = 0$ for all $n < n_0$ then $y[n] = 0$ for all $n < n_0$, and all the required initial conditions $IC[n_0]$ are zero. \square

Henceforth we shall make the two assumptions of Theorem 3 for systems described by (46). There are two major subclasses of such DTI systems: *Finite impulse response (FIR)* DTI systems, when $a_k = -\infty$ for all k . Then (46) has no recursive part, and the impulse response

$$g[n] = \begin{cases} b_n & \text{if } n = 0, 1, \dots, M, \\ -\infty & \text{if } n < 0, n > M \end{cases} \quad (52)$$

has finite support. All these systems are stable. This class is identical with the class of all morphological dilations with finite-support structuring elements. *Infinite impulse response (IIR)* DTI systems, when $a_k \neq -\infty$ for at least one k . The example of the first-order system (47) demonstrates that such systems have an impulse response of infinite support. The stability of the IIR systems is governed by Theorem 1(d).

4.1. Recursive DTI systems

In the rest of this section we shall deal with a standard autoregressive form of (46),

$$y[n] = \max\{y([n-1]) + a_1, \dots, y(n-N) + a_N, x[n]\}, \quad (53)$$

which is obtained by pre-dilating the input signal x with the finite-support signal b defined as $b[n] = b_n$ for $n = 0, \dots, M$ and $-\infty$ else. We also assume that $b_0 = 0$, because a nonzero b_0 only adds a constant b_0 to the output y . Thus, in the standard autoregressive form we ignore the non-recursive part of the dilation (which is understood quite well from the existing theory and geometric intuition about dilations by finite-support structuring elements) and focus only on the recursive part.

First-order system: From the general solution of (47), if a system is described by

$$y[n] = \max(y[n-1] + a_1, x[n]), \quad (54)$$

its impulse response is $g[n] = a_1 n + s[n]$. The upper slope transform of g , and hence the system's slope response is

$$G(\alpha) = -s(\alpha - a_1) = \begin{cases} +\infty, & \alpha < a_1, \\ 0, & \alpha \geq a_1, \end{cases} \quad (55)$$

It acts as a 'slope high-pass' filter since it passes from the input signal only those segments whose slopes are $\geq a_1$. In general, the higher the value of $G(\alpha)$ is, the more deemphasized the input's components with slope α become in the output. For example, $G(\alpha) = \infty$ means that the component with slope α is completely rejected, whereas a value $G(\alpha) = 0$ passes this slope completely unchanged.

Nth-order system: Finding a closed-formula expression for the impulse response is generally difficult³ for $N > 1$. Thus, we shall first find the slope response G and then, via inverse slope transform,

³The impulse response of a second-order ($N = 2$) causal system described by (53) is found by induction to be

$$g[n] = a_1 n + \max(0, (a_2 - 2a_1) \lfloor n/2 \rfloor) + s[n].$$

For $N \geq 3$ finding g by induction becomes too meshy.

find the impulse response g or its envelope \hat{g} . Applying \mathcal{A}_\vee to (53) yields

$$\begin{aligned} Y(\alpha) &= G(\alpha) + X(\alpha) \\ &= \left(\bigvee_{k=1}^N X(\alpha) + G(\alpha) - k\alpha + a_k \right) \vee X(\alpha). \end{aligned} \quad (56)$$

Assuming that $X(\alpha)$ is finite yields

$$\begin{aligned} G(\alpha) &= \max\{G(\alpha) - \alpha + a_1, \dots, \\ &G(\alpha) - N\alpha + a_N, 0\}. \end{aligned} \quad (57)$$

Thus, $G(\alpha) \geq 0$. A nontrivial (i.e., different than ∞) solution G is obtained as follows: Let

$$\alpha_0 = \max_k \frac{a_k}{k}.$$

If $\alpha \geq \alpha_0$, then $a_k - k\alpha \leq 0$ for all k . Hence a solution is $G(\alpha) = 0$. Now if $\alpha < \alpha_0$, then $a_k - k\alpha > 0$ for some k , and assume that $a_m - m\alpha \geq a_k - k\alpha$ for all such k . Then $G(\alpha)$ must satisfy the equality $G(\alpha) = G(\alpha) - m\alpha + a_m$. This implies $G(\alpha) = \infty$. Thus the slope response is

$$G(\alpha) = -s(\alpha - \alpha_0). \quad (58)$$

Applying \mathcal{A}_\vee^{-1} to G yields the upper envelope \hat{g} of the impulse response

$$\hat{g}[n] = \alpha_0 n + s[n] \geq g[n]. \quad (59)$$

Examples of g for three different sequences $\{a_k\}$ are given in Fig. 6, where for the cases (a), (b) and (c) we have $\alpha_0 = 0, 0.2$ and -0.2 , respectively, and the upper envelope \hat{g} is the half-line $\alpha_0 n + s[n]$. Outputs of recursive DTI systems using various $\{a_k\}$ are shown in Fig. 7. It is evident from Figs. 6 and 7 that, although over short time periods g has the shape induced by the sequence $\{a_k\}$ and dominates the output of the recursive DTI system during time periods when the slope of the input signals is smaller than α_0 , over long time scales it behaves like its upper envelope \hat{g} . It is also interesting to note that by appropriately choosing the coefficients $\{a_k\}$ we can give the local variations of g many different patterns. For instance, many choices of $a_k < 0$ for all $k < N$ and $a_N = 0$ make g periodic; such examples include the triangle sequence

$a_k = |k - N/2| - N/2$ (for even N) in the case of Fig. 6(a) which creates a periodic negative triangle train for g , the sine sequence $a_k = -\sin(\pi k/N)$ which produces a (negative rectified) sine wave as impulse response $g[n] = -|\sin(\pi n/N)|$, and numerous others.

In general, the analysis for first-order recursive systems is simple: their impulse response g is a causal line and it is simple to understand the system's behavior in the time domain as a dilation by a half-line. Their slope response (obtained from applying the slope transform on g) tells us that the system behaves as a slope high-pass filter. Although the insight from the slope domain is intrinsically interesting, it is not necessary because we can understand the system's behavior entirely in the time domain.

However, for N th-order systems with $N > 1$ the slope domain analysis is necessary to understand the long-time dynamics of these systems. Finding the impulse response in the time domain is generally complicated and unintuitive. By contrast, our result in (58) offers a simple formula for the slope response. This turned out identical to the slope response of the first-order system, i.e., an ideal-cutoff slope-selective filter. Applying the inverse slope transform also informs us that the upper envelope \hat{g} of the impulse response is a causal line with slope $\alpha_0 = \max_k \{a_k/k\}$. Together G and \hat{g} can describe the large-time dynamics of the system since they predict a long-time behavior equivalent to a first-order system whose cutoff slope is α_0 . By 'long' here we mean much longer than the length N of the coefficient sequence $\{a_k\}$. In addition, if g is a line, then the above analysis is also exact for the short-time behavior.

4.2. Slope filters and envelope estimation

Consider the causal recursive DTI system $y_1[n] = \max(y_1[n-1] + a_1, x[n])$ with $a_1 < 0$, which is a morphological dilation of the input by the semi-infinite line $g_1[n] = a_1 n + s[n]$. The output $y_1[n]$ is constrained to be $\geq x[n]$ for all n and hence provides a type of upper envelope of $x[n]$. As Fig. 8(b) shows, when computing y_1 in forward

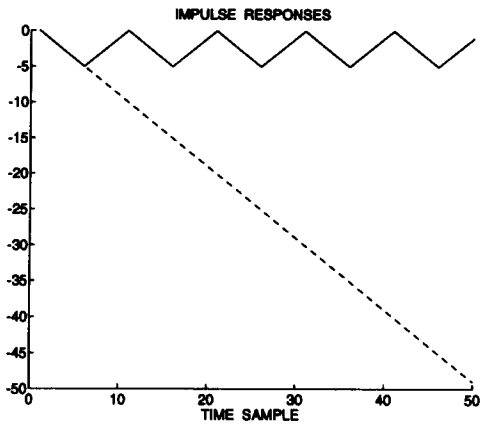
time, during periods where the envelope peaks keep decreasing y_1 falls linearly with slope a_1 in between these consecutive peaks. When the envelope peaks start increasing, y_1 continues to fall between peaks, whereas it should rise. This can also be understood in the slope domain where the slope response of this system is $G_1(\alpha) = -s(\alpha - a_1)$ and hence rejects all negative slopes $< a_1$ but passes all other slopes. To be able to also reject some positive slopes we must pass the input through an anti-causal system $y_2[n] = \max(y_2[n+1] + a_2, x[n])$ with $a_2 > 0$. Fig. 8(c) shows the output envelope y_2 when this system is run backwards in time. It corresponds to a morphological dilation of the input by the anti-causal line $g_2[n] = a_2 n + s[-n]$. Its slope response is $G_2(\alpha) = -s(a_2 - \alpha)$ and hence it rejects all positive slopes $> a_2$. To symmetrize this process we can take the maximum $y = y_1 \vee y_2$ of the two envelopes as the final estimated upper envelope of the input, which is shown in Fig. 8(d). The mapping $x \mapsto y$, i.e., the maximum of two DTI systems, is another DTI system with overall impulse response $g = g_1 \vee g_2$ and overall slope response $G = G_1 \vee G_2$. Thus,

$$g[n] = \begin{cases} a_1 n, & n \geq 0 \\ a_2 n, & n \leq 0 \end{cases} \xleftrightarrow{\mathcal{S}_\vee} G(\alpha) = \begin{cases} 0, & a_1 \leq \alpha \leq a_2 \\ +\infty, & \text{else.} \end{cases} \quad (60)$$

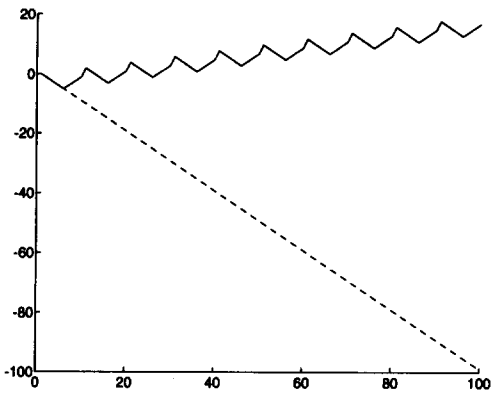
To design a *symmetric* ideal-cutoff slope filter we select $a_2 = -a_1 = \alpha_0 > 0$ which passes slopes with magnitude $\leq \alpha_0$ unchanged and rejects all other slopes. This is the case in Fig. 8(d). However, if we let a_1, a_2 be arbitrary real numbers with the only constraint that $a_1 < a_2$, then the filter in (60) becomes the most general *ideal slope bandpass filter*. It passes unchanged all input slopes within the interval $[a_1, a_2]$ and rejects the rest. As we saw above, it corresponds to a morphological dilation of the input by an infinite conical structuring element. In discrete time, it can be easily realized as the maximum of a causal and anti-causal recursive first-order dilation.

Consider now the problem of envelope detection in amplitude-modulated (AM) signals

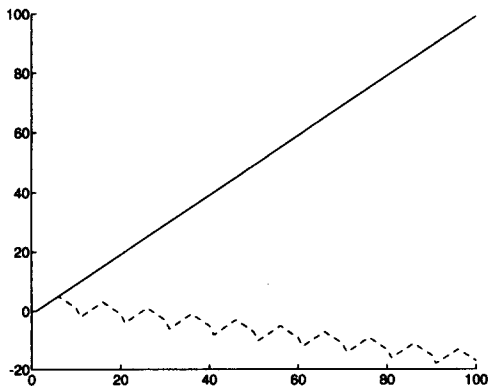
$$x_{AM}(t) = [1 + \lambda \cos(\omega_a t)] \cos(\omega_c t), \quad \omega_a \ll \omega_c.$$



(a)

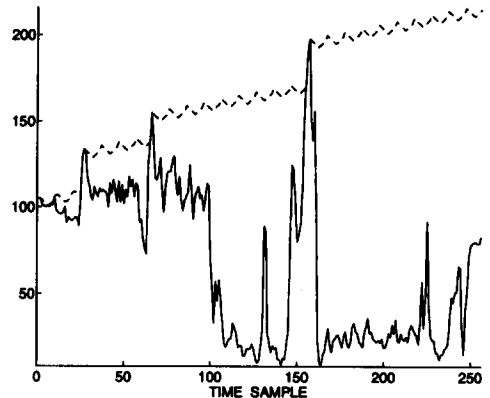


(b)

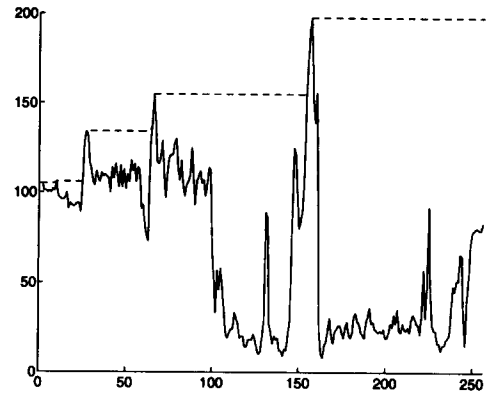


(c)

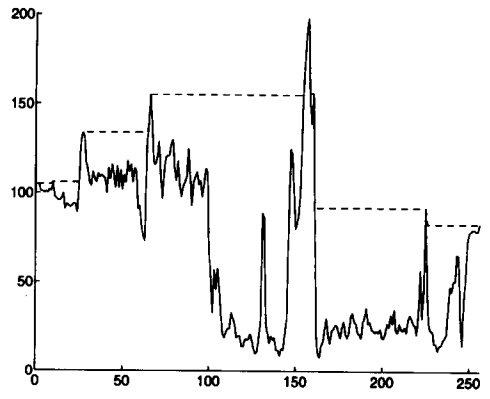
Fig. 6. Impulse responses of tenth-order recursive DTI (solid upper line) and ETI (dashed lower line) systems for various coefficient sequences $\{a_k\}$. (a) $a_k = |k - 5| - 5, k = 1, \dots, 10$. (b) $a_k = |k - 5| - 5, k = 1, \dots, 9$ and $a_{10} = 2$. (c) $a_k = 5 - |k - 5|, k = 1, \dots, 9$ and $a_{10} = -2$; i.e., a_k are the negatives of the ones in (b).



(a)



(b)



(c)

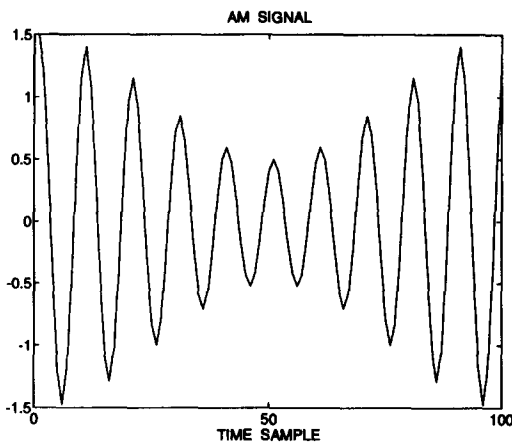
Fig. 7. (a) Signal x (solid line) and its output (dashed line) from the recursive DTI system with the coefficients of the example of Fig. 6(b). (b) Signal x and its output from system $y(n) = \max[y(n-1), x(n)]$ in forward time. (c) Min of outputs of system in (b) computed in forward and backward time.

Fig. 8(a) shows one period of a sampled AM signal $x[n] = x_{AM}(nT)$, where T is sampling period, with $\omega_a T = \pi/50$, carrier $\omega_c T = \pi/5$, and modulation index $\lambda = 0.5$. As illustrated in Fig. 8(b)–(d), we have applied the previous ideas on recursive DTI systems to estimating the upper envelope of an AM signal as the maximum of the outputs from a causal and anti-causal system, each described by $y[n] = \max(y[n \pm 1] \pm \alpha_0, x[n])$. To maximize the smoothness of the resulting envelope we selected the slope parameter α_0 to match the average slope of

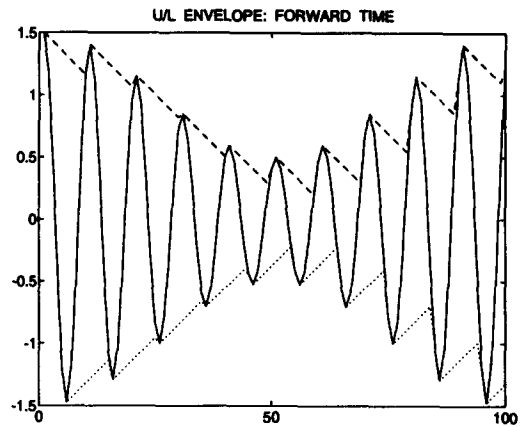
the true envelope $f(t) = [1 + \lambda \cos(\omega_a t)]$ within time intervals equal to the carrier period $2\pi/\omega_c$. To avoid dependency on the location of such time intervals we also averaged over one-half the period of $f(t)$, where $df/dt \leq 0$. This yielded

$$\alpha_0 = \frac{2\lambda\omega_c T \sin[2\pi(\omega_a/\omega_c)]}{\pi^2},$$

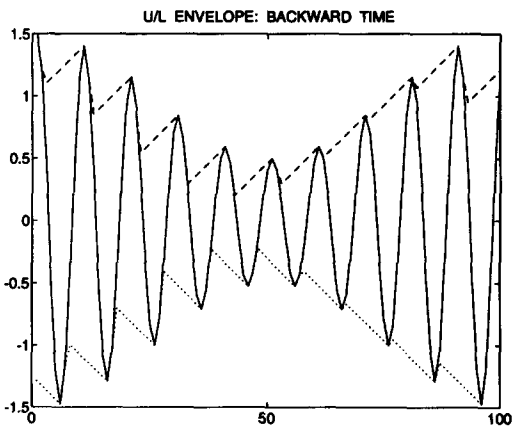
which has the value $\alpha_0 = 0.0374$ for the example of Fig. 8. For envelope signals more general than a cosine, the same formula may be applicable if ω_a is the



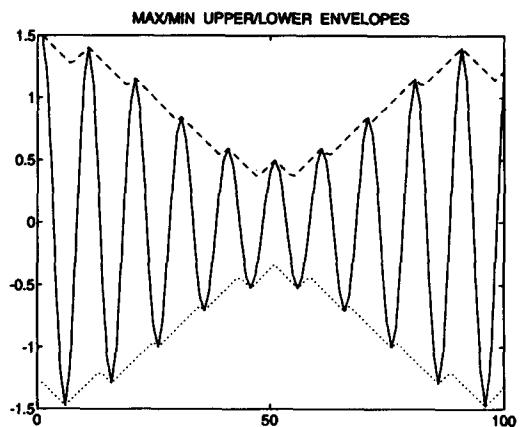
(a)



(b)



(c)



(d)

Fig. 8. Envelope estimation in AM signals. Upper envelopes (dashed lines) are outputs from recursive DTI systems. Lower envelopes (dotted lines) are outputs from recursive ETI systems. The envelopes are generated in (b) by running the recursion forward in time, in (c) backward in time, and in (d) by taking the maximum (respectively minimum) of the two upper (respectively lower) envelopes from (b) and (c).

bandwidth of the envelope. It remains to be seen whether the above choice of α_0 is optimal according to some criterion. An alternative approach would be to adapt α_0 based on previous input and output slopes, e.g., as some function of $x[n] - x[n-1]$ and/or $y[n-1] - y[n-2]$.

The efficiency of first-order recursive DTI or ETI systems to estimate signal envelopes and their extremely small complexity (two additions and three comparisons per output sample) makes them promising for AM detection and other applications of envelope detection.

Since first-order recursive DTI systems are capable of envelope estimation and systems of a larger order $N > 1$ behave effectively as first-order systems, the following question arises: Do we ever need recursive DTI systems with order $N > 1$? One case with a 'yes' answer is when we apply them to estimating envelopes of noisy signals, because then their outputs would follow the envelope peaks of both the signal and the noise. A solution for this case is to replace the maximum operation in a general DTI system described by (46) with a more general rank operation. This yields systems described by the nonlinear equation

$$y[n] = r^{\text{th}} \text{rank} \{ \{ y[n-k] + a_k; k = 1, \dots, N \} \cup \{ x[n-m] + b_m; m = 0, \dots, M \} \}, \quad (61)$$

where $r = 1, \dots, N + M + 1$. These recursive rank systems are a generalization of the recursive rank-order filters (4) studied in [12] which correspond to a special case with $a_k = 0$, $b_m = 0$ and $M = N$. If we rank the weighted samples in descending order, then $r = 1$ corresponds to the max equation (46), and $r = N + M + 1$ corresponds to a dual min equation studied later. For ranks r around the middle value $(N + M + 1)/2$ the recursive system performs some nonlinear smoothing of the median type, and this could reduce the noise in the envelope estimation.⁴ Now, as shown in [10], any rank operation can be obtained as the minimum of the maxima of several subsets of the original

window of input/output samples. Thus, the above recursive rank systems can be realized as the minimum of several recursive DTI systems whose order is $\leq N + M + 1$.

5. Max differential equation

First-order discrete DTI systems described by the max difference equation (54) behave as slope-selective filters with ideal-cutoff slope response $G(\alpha) = -s(\alpha - a_1)$. Can we find continuous-time systems with the same slope response? Next we present a nonlinear differential equation which describes the time dynamics of a system with the above slope response.

In the time domain such a system would correspond to a morphological dilation by a causal line $g(t) = -\alpha_0 t + s(t)$. Let $\alpha_0 > 0$. From Fig. 8(b) we can imagine that dilating a signal $x(t)$ by the half-line $g(t)$ produces a type of upper envelope where, scanning toward the positive time direction, all the parts of the signal with slope larger than $-\alpha_0$ remain unchanged, whereas parts with slope smaller than $-\alpha_0$ are covered by line of slope $-\alpha_0$ which extends until a point of the signal graph with slope larger than $-\alpha_0$, after which time the same pattern repeats. The dynamics of this dilation are described by the following nonlinear differential equation:

$$y(0) = x(0),$$

$$y'(t+) = \begin{cases} \max(x'(t+), -\alpha_0) & \text{if } y(t) = x(t), \\ -\alpha_0 & \text{if } y(t) > x(t), \end{cases} \quad (62)$$

where $x'(t+) = \lim_{p \downarrow 0} [x(t+p) - x(t)]/p$. The reason for using right-sided derivatives is twofold: (i) they are sufficient to create the forward dynamics, and (ii) the input and mostly the output signal might not possess a two-sided derivative at all points. Note that, when $y(t) > x(t)$ then the output derivative $y'(t) = y'(t+) = -\alpha_0$ exists. Obviously, the solution of (62) is $y(t) = x(t) \oplus g(t)$.

It is interesting to note that replacing derivatives in (62) with simple one-sample differences transforms the max differential equation into the first-order max

⁴In [12] a figure example is shown on detecting the envelope of a noisy AM signal by a nonrecursive rank filter of the type $y[n] = 2\text{nd rank}\{x[n-k]; |k| \leq 4\}$.

difference equation. Specifically, if we replace continuous time t with discrete nT and

$$x(t) \mapsto x[n],$$

$$x'(t+) \mapsto (x[n+1] - x[n])/T,$$

$$y'(t+) \mapsto (y[n+1] - y[n])/T,$$

then (62) becomes as follows: If $y(t) = x(t)$, then $y[n] = x[n]$ and

$$y[n+1] - y[n] = \max(x[n+1] - x[n], -\alpha_0 T),$$

which implies

$$y[n+1] = \max(y[n] - \alpha_0 T, x[n+1]).$$

If $y(t) > x(t)$, then $y[n] > x[n]$ and $y[n] - y[n-1] = -\alpha_0 T$; hence

$$\begin{aligned} y[n] &= \max(y[n], x[n]) \\ &= \max(y[n-1] - \alpha_0 T, x[n]). \end{aligned} \quad (63)$$

Thus, (62) is the continuous-time counterpart of (63).

6. Erosion translation-invariant (ETI) systems

A signal operator $\mathcal{E}: x \mapsto y$ is called an *erosion translation-invariant (ETI)* (system) if it is a lattice erosion, i.e., distributes over any infimum of inputs, and is translation invariant. Equivalently, it is ETI if it obeys a morphological *infimum superposition*

$$\mathcal{E} \left[\bigwedge_i c_i + x_i(t) \right] = \bigwedge_i c_i + \mathcal{E}[x_i(t)] \quad (64)$$

and is time-invariant. It turns out that the prototype ETI system is based on a morphological erosion, which is the dual of the dilation with respect to signal negation. Thus, ETI systems are duals of DTI systems, and their properties can be easily deduced from our previous discussion. Next we briefly outline the main ideas for their analysis in the time and slope domain.

6.1. Time domain

The *support* of signals $x: \mathbb{E} \rightarrow \bar{\mathbb{R}}$ analyzed via ETI systems is defined as $\text{Spt}(x) = \{t: x(t) < \infty\}$. If we

use the signal $-\mu(t)$ as the zero impulse, then the *impulse response* of an ETI system \mathcal{E} is defined as the signal $f = \mathcal{E}(-\mu)$. By working as in Theorem 1, the following can be shown.

Theorem 4. A system \mathcal{E} with $f = \mathcal{E}(-\mu)$ is

(i) *ETI* iff

$$\begin{aligned} \mathcal{E}[x(t)] &= x(t) \ominus (-f(-t)) \\ &= \bigwedge_{\tau} x(\tau) + f(t - \tau). \end{aligned} \quad (65)$$

(ii) *Causal* iff $f(t) = \infty \quad \forall t < 0$.

(iii) *Anti-causal* iff $f(t) = \infty \quad \forall t > 0$.

(iii) *Stable* iff $\sup\{|f(t)|: t \in \text{Spt}(f)\} < \infty$.

Thus, ETI systems are completely determined by their impulse response f since they correspond to a morphological erosion by the negated reflection of f .

6.2. Slope domain

The affine signals $x(t) = \alpha t + b$ are eigenfunctions of any ETI system \mathcal{E} because the corresponding outputs are

$$\mathcal{E}[\alpha t + b] = \alpha t + b + F(\alpha) \quad (66)$$

where the corresponding eigenvalue

$$F(\alpha) = \bigwedge_t f(t) - \alpha t \quad (67)$$

is the lower slope transform of the impulse response $f = \mathcal{E}(-\mu)$. We call $F(\alpha)$ the slope response of the ETI system because it is added to the intercept of any input line with slope α . It plays an important role in the analysis of ETI systems in the slope domain since the lower slope transform of any output signal is the sum of the input slope transform and the system's slope response:

$$\begin{aligned} y(t) &= x(t) \ominus (-f(-t)) \xrightarrow{\mathcal{E}} \\ Y_{\wedge}(\alpha) &= X_{\wedge}(\alpha) + F(\alpha). \end{aligned} \quad (68)$$

6.3. Min difference equations

We focus now on signals $x, y: \mathbb{Z} \rightarrow \mathbb{R} \cup \{\infty\}$ analyzed via discrete systems described by the following min difference equation:

$$y[n] = \left(\bigwedge_{k=1}^N a_k + y[n-k] \right) \wedge \left(\bigwedge_{m=0}^M b_m + x[n-m] \right) \quad (69)$$

for which we henceforth assume that (i) whenever $x[n] = \infty$ for all $n < n_0$ then $y[n] = \infty$ for all $n < n_0$, where n_0 is an arbitrary but otherwise fixed time instant, and (ii) the required initial conditions $IC(n_0)$ are ∞ . This guarantees that (69) describes a causal ETI system.

Let us return to (69) describing an ETI system and assume that $b_0 = 0$ and $b_m = \infty$ for $m > 0$.

First-order system: If $N = 1$, then the impulse and slope response are

$$f[n] = a_1 n - s[n] \xrightarrow{\mathcal{A}_\wedge} F(\alpha) = s(a_1 - \alpha). \quad (70)$$

Thus this system acts as an ideal *slope low-pass filter* since it eliminates all linear trends in the input whose slope is $> a_1$ and passes all other slopes unchanged.

For an *Nth-order* system with $N > 1$, applying \mathcal{A}_\wedge to (69) and solving for F yields

$$F(\alpha) = \min[F(\alpha) - \alpha + a_1, \dots, F(\alpha) - N\alpha + a_N, 0]. \quad (71)$$

Thus

$$F(\alpha) = s(\alpha_0 - \alpha), \quad \alpha_0 = \min_k \frac{a_k}{k} \quad (72)$$

and the convex lower envelope of f is $f[n] = \alpha_0 n - s[n]$. Thus a recursive *Nth-order* ETI system behaves, over time scales longer than N , effectively as a first-order system. Examples of the impulse response f of ETI systems described by a tenth-order min difference equation are shown in Fig. 6.

6.4. Envelope estimation

Whatever we discussed for recursive DTI systems and their ability to estimate envelopes of the input signals also extends to ETI systems with only a few minor changes. A continuous-time ETI system with a symmetric slope response

$$F(\alpha) = \begin{cases} 0, & |\alpha| \leq \alpha_0, \\ -\infty, & |\alpha| > \alpha_0 \end{cases} \quad (73)$$

acts as an ideal-cutoff slope bandpass filter with impulse response

$$f(t) = \alpha_0 |t|, \quad \alpha_0 > 0. \quad (74)$$

This ETI system yields as output a lower envelope of the input signal where all slopes absolutely higher than α_0 are rejected and the rest pass unchanged. The corresponding DTI system with impulse response $g(t) = -\alpha_0 |t|$ generates an upper envelope of the input signal. As for the DTI system, the above ETI system can be realized by taking the minimum of the outputs of two ETI systems, one with causal impulse response $\alpha_0 t + s(t)$ and the other with anti-causal impulse response $-\alpha_0 t + s(-t)$. Each such system can be realized in the time domain either via eroding the input by a half-line or by running a dynamical system based on a min differential equation resulting from (62) by replacing the max, $>$ and $-\alpha_0$ with min, $<$ and α_0 . In discrete time, this differential equation becomes a first-order recursive min equation. Examples are shown in Fig. 8 where the lower envelopes are generated by recursive systems $y[n] = \min(y[n \mp 1] \pm \alpha_0, x[n])$ run in forward and backward time.

Finally, note that the DTI (respectively ETI) systems described by the first-order max (respectively min) differential/difference equation or equivalently via a morphological dilation (respectively erosion) by a line is actually a *closing* (respectively opening) in the lattice-theoretic sense because it is idempotent, extensive (respectively anti-extensive) and increasing. The same is true for both their causal and anti-causal systems, as well as for their max (respectively min) superpositions in the case of DTI (respectively ETI) systems. We call them *envelope closing* and *envelope opening*, and they are actually morphological

dilations and erosions by infinite line or conical structuring elements.

References

- [1] G. Borgefors, "Distance transformations in arbitrary dimensions", *Comput. Vision Graph. Image Process.*, Vol. 27, 1984, pp. 321–345.
- [2] H.B. Callen, *Thermodynamics and an Introduction to Thermostatistics*, Wiley, New York, 1985, Chapter 5.
- [3] R. Courant and D. Hilbert, *Methods of Mathematical Physics*, Wiley, New York, 1962.
- [4] L. Dorst and R. van den Boomgaard, "An analytical theory of mathematical morphology", in *Proc. 1st Internat. Workshop on Mathematical Morphology and its Application to Signal Processing*, Univ. Politecnica de Catalunya, Barcelona, Spain, May 1993.
- [5] H.J.A.M. Heijmans and C. Ronse, "The algebraic basis of mathematical morphology. Part I: Dilations and erosions", *Comput. Vision Graph. Image Process.*, Vol. 50, 1990, pp. 245–295.
- [6] D. Keller, "Reconstruction of STM and AFM images distorted by finite-size tips", *Surface Sci.*, Vol. 253, 1991, pp. 353–364.
- [7] B. Lay, "Recursive algorithms in mathematical morphology", *Acta Stereol.*, Vol. 6/III, 1987, pp. 691–696.
- [8] P. Maragos, "Max–min difference equations and recursive morphological systems", in *Proc. 1st Internat. Workshop on Mathematical Morphology and its Application to Signal Processing*, Univ. Politecnica de Catalunya, Barcelona, Spain, May 1993.
- [9] P. Maragos, "Slope transforms: Theory and application to nonlinear signal processing", *IEEE Trans. Signal Process.*, submitted; also Tech. Report 93-1, DSP Lab, Georgia Inst. Technology, December 1993.
- [10] P. Maragos and R.W. Schafer, "Morphological filters – Parts I and II", *IEEE Trans. Acoust. Speech Signal Process.*, Vol. 35, August 1987, pp. 1153–1184.
- [11] P. Maragos and R.W. Schafer, "Morphological Systems for Multidimensional Signal Processing", *Proc. IEEE*, Vol. 78, April 1990, pp. 690–710.
- [12] T.A. Nodes and N.C. Gallagher, "Median filters: Some modifications and their properties", *IEEE Trans. Acoust., Speech Signal Process.*, Vol. 30, October 1982, pp. 739–746.
- [13] A.V. Oppenheim and R.W. Schafer, *Discrete-time Signal Processing*, Prentice-Hall, Englewood Cliffs, NJ, 1988.
- [14] A.V. Oppenheim and A.S. Willsky with I.T. Young, *Signals and Systems*, Prentice-Hall, Englewood Cliffs, NJ, 1983.
- [15] A. Rosenfeld and J.L. Pfaltz, "Sequential operations in digital picture processing", *J. ACM*, Vol. 13, October 1966, pp. 471–494.
- [16] J. Serra, *Image Analysis and Mathematical Morphology*, Academic Press, New York, 1982.
- [17] J. Serra, ed., *Image Analysis and Mathematical Morphology, Vol. 2: Theoretical Advances*, Academic Press, New York, 1988.
- [18] S.R. Sternberg, "Grayscale morphology", *CVGIP*, Vol. 35, 1986, pp. 333–355.
- [19] J. van Tiel, *Convex Analysis*, Wiley, New York, 1984.